PARAMETRIC ANALYSIS OF AN ALKALINE MEMBRANE FUEL CELL

Lauber de Souza Martins[1], martins@caps.fsu.edu
Elise Meister Sommer[2], elise.sommer@gmail.com
Juan Carlos Ordonez[1], ordonez@eng.fsu.edu
José Viriato Coelho Vargas[1], jvargas@demec.ufpr.br

1 Department of Mechanical Engineering and Center for Advanced Power Systems, Florida State University, Tallahasse, Florida 32310-6046, USA

2 Universidade Federal do Paraná – UFPR. Bloco IV do Setor de Tecnologia, Centro Politécnico (Campus II), Bairro Jardim das Américas Cx. 19011, CEP 81531-990, Curitiba, PR Brasil

Abstract. *The mathematical model developed and experimentally validated on previous works for the Alkaline Membrane Fuel Cell (AMFC) can be used to simulate the fuel cell performance as a function of different parameters. The resulting equations from the mathematical model were solved with a Fortran code using a quasi-Newton method. The influence of important design parameters as the porosity of the reactive layer of electrodes and of the membrane and operational parameters (temperature of the feeding gases) on the AMFC power output is studied and discussed in this paper. These results can be used as future tool for power optimization.*

Keywords*: Alkaline Membrane Fuel Cell, Numerical Simulation, Parametric Analysis*

1. INTRODUCTION

The Alkaline Membrane Fuel Cell (AMFC) is a recently developed fuel cell type with a liquid alkaline electrolyte , different than other fuel cell types. The membrane is made of a solid and porous support soaked on a potassium hydroxide solution. This is why the new type of fuel cell was named AMFC – Alkaline Membrane Fuel Cell.

Numerical simulations are used in this paper to obtain the influence on AMFC performance of design and operational parameters. The performance parameter evaluated in this paper was the fuel cell net power output.

It also considered how the temperature and molarity affect the ionic conductivity of the electrolyte.

2. MATHEMATICAL MODEL

A schematic diagram of the internal structure of a AMFC is shown in Fig. 1 and Fig. 2. Pure hydrogen and pure oxygen are considered in this analysis as fuel and oxidant respectively. The fuel cell was divided into seven control volumes that interact energetically with one another and with the ambient. Two bipolar plates were added with the function of allowing the electrons produced by the electrochemical oxidation reaction at the anode to flow to the external circuit.

The model consists of the conservation equations for each control volume, and equations accounting for electrochemical reactions, where they are present. The reversible electrical potential and power of the fuel cell are then computed as functions of the temperature and pressure fields determined by the model. The actual electrical potential and power of the fuel cell are obtained by subtracting from the reversible potential the losses due to surface overpotentials, slow diffusion and all internal ohmic losses through the cell. These are functions of the total cell current (I), which is directly related to the external load. In this model, the total current is considered an independent variable.

The control volumes (CV) are fuel channel (CV1), the anode diffusion-backing layer (CV2), the anode reaction layer (CV3), the alkaline membrane (CV4), the cathode reaction layer (CV5), the cathode diffusion backing layer (CV6) and the oxidant channel (CV7).

Dimensionless variables are defined based on the geometric and operating parameters of the system. Pressures and temperatures are referenced to ambient conditions: $P_i = p_i / p_\infty$ and $\theta_i = T_i / T_\infty$, where P is the dimensionless pressure, p is the pressure, N/m^2 ; θ is the dimensionless temperature, T is the temperature, K; the subscript i and ∞ represent the substance or a location in the fuel cell and the ambient respectively. Other dimensionless variables are defined as:

$$\psi = \frac{\dot{m}_i}{\dot{m}_{ref}} \tag{1}$$

$$N_i = \frac{U_{wi} V_T^{2/3}}{\dot{m}_{ref} c_{p,f}}, \quad \tilde{A}_i = \frac{A_i}{V_T^{2/3}} \tag{2}$$

where ψ and $\dot{m}$ are the dimensionless mass flow rate and mass flow rate kg/s, respectively; N is the dimensionless global wall heat transfer coefficient, U is the global wall heat transfer coefficient, W/m^{2}K; V_T is the total volume of the fuel cell, m^3; $c_{p,f}$ is the specific heat at constant pressure of the fuel, kJ/kgK; $\tilde{A}$ is the dimensionless area, A is the area, m^2; the subscript i indicates a substance or a location in the fuel cell, ref indicate the reference level and w indicates wall.

$$\xi_j = \frac{L_j}{V_T^{1/3}} \tag{3}$$

where L indicates the length, m; ξ is the dimensionless length ;the subscript j indicates a particular dimension of the fuel cell geometry, Fig. 2.

$$\tilde{h} = \frac{hV_T^{2/3}}{\dot{m}_{ref} c_{p,f}}, \qquad \tilde{k} = \frac{kV_T^{1/3}}{\dot{m}_{ref} c_{p,f}} \tag{4}$$

Where h is the heat transfer coefficient, W/m^{2}K; k is the thermal conductivity, W/mK; $\tilde{h}$ s the dimensionless heat transfer coefficient, $\tilde{k}$ is the dimensionless thermal conductivity.

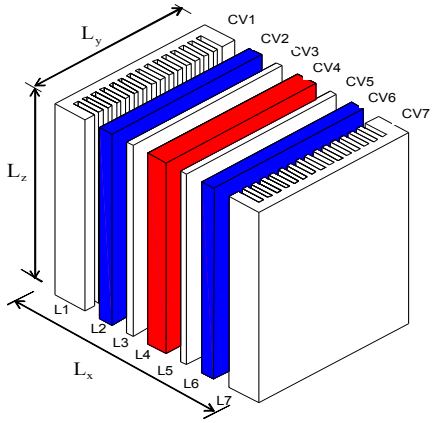

Figure 1. Single AMFC fuel cell model and control volumes distribution, L is the length of each CV, Lx is the total length of the fuel cell, Lz is the high and Ly is the width of the fuel cell

The hydrogen mass flow rate required for the current (I) dictated by the external load is

$$\dot{m}_{H_2} = \dot{n}_{H_2} M_{H_2} = \frac{I}{nF} M_{H_2} \tag{5}$$

Where $\dot{n}$ is the molar flow rate, kmol/s; M is the molar weight,kg/kmol; n is the equivalent electron per mole of reacthat, eq/mol; I is the total current, A; F is the Faraday constant, C/eq.

Therefore, the oxygen mass flow rate needed for a AMFC fuel cell is

$$\dot{m}_{O_2} = \frac{1}{2} \dot{n}_{H_2} M_{O_2} \tag{6}$$

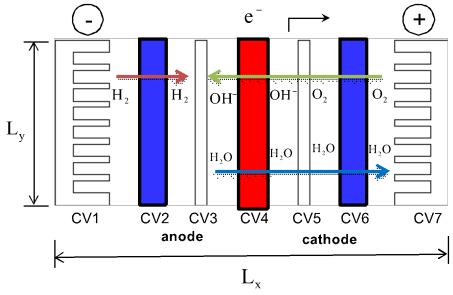

Figure 2. Upper view of the control volumes of a single AMFC

2.1. Energy conservation

The wall heat transfer area of one control volume in the AMFC is $A_{wi} = \tilde{p}_s L_i \ (2 \le i \le 6)$and $A_{wi} \cong \tilde{p}_s L_i + L_y L_z$ (i = 1,7;), where $\tilde{p}_s = 2(L_y + L_z)$ is the perimeter of the fuel cell cross-section. The control volumes are $V_j = L_y L_z L_j$ $(2 \le j \le 6)$and $V_j = n_c L_c L_l L_z$ (j =1, 7), where n_c is the integer part of $L_y/(L_t + L_c)$, i.e., the number of parallel ducts in each gas channel (fuel and oxidant). The mass and energy balances for CV1 yield the temperature in CV1,

$$\tilde{Q}_{w1} + \psi_f(\theta_f - \theta_1) + \tilde{Q}_{12} + \tilde{Q}_{lohm} = 0 \tag{7}$$

and

$$\tilde{Q}_{wi} = N_i \tilde{A}_{wi}(1-\theta_i), \ \tilde{Q}_{iohm} = I^2 \beta_i / (\dot{m}_{ref} c_{p,f} T_\infty) \tag{8}$$

where $\tilde{Q}_{12} = \tilde{h}_1 \tilde{A}_s (1-\phi_2)(\theta_2 - \theta_1)$, $\tilde{A}_s = L_y L_z / V_T^{2/3}$. Subscript i represents a location in the cell, i.e., a particular CV, f indicates fuel, ohm indicates ohmic and ϕ the porosity. The dimensionless heat transfer rates for all the compartments are $\tilde{Q}_i = \dot{Q}_i / \dot{m}_{ref} c_{p,f} T_\infty$. The subscript i accounts for any of the heat transfer interactions that are present in the model. $\dot{Q}$ is the heat transfer rate, W; $\tilde{Q}$ is the dimensionless heat transfer rate, β is the electrical resistance, Ω.

Assuming that the channels are straight and sufficiently slender, and using the ideal gas model, the pressure drops are

$$\Delta P_i = f_i \left(\frac{\xi_z}{\xi_i} + \frac{\xi_z}{\xi_c} \right) \frac{P_j}{\theta_i} \frac{R_f}{R_i} \tilde{u}_i^2 \tag{9}$$

where i = 1,7 and j = f (fuel), ox (oxidant), respectively. Here $\tilde{u}_i = (\tilde{u}_{i,in} + \tilde{u}_{i,out})/2$ is the channel dimensionless mean velocity, defined as $\tilde{u} = u/(R_f T_\infty)^{1/2}$, and f is the friction factor, ξ_c is the dimensionless width of the gas channels, R is the ideal gas constant kJ/kgK. According to mass conservation, the dimensionless mean velocities in the gas channels are

$$\tilde{u}_1 = \frac{C\theta_1}{\tilde{A}_{c1} P_f} \left[\psi_f - \frac{\psi_{H_2}}{2} \right] \tag{10}$$

$$\tilde{u}_7 = \frac{R_{ox} C \theta_7}{R_f \tilde{A}_{c7} P_{ox}} \left[\psi_{ox} - \frac{\psi_{O_2}}{2} \right] \tag{11}$$

$$C = \frac{(R_f T_\infty)^{1/2} \dot{m}_{ref}}{p_\infty V_T^{2/3}} \tag{12}$$

where $\tilde{A}_{ci} = n_c L_c L_i / V_T^{2/3}$, i = 1,7 and L_c is the width of the gas channel, m.

For the laminar regime, $\mathrm{Re}_{D_h} < 2300$ (Shah and London, 1978):

$$f_i \, \mathrm{Re}_{Dh,j} = 24(1 - 1.3553\delta_i + 1.9467\delta_i^{\,2} - 1.7012\delta_i^3 + 0.9564\delta_i^4 - 0.2537\delta_i^5) \tag{13}$$

$$\frac{h_i D_{h,i}}{k_i} = 7.541(1 - 2.610\delta_i + 4.970\delta_i^{\,2} - 5.119\delta_i^3 + 2.702\delta_i^4 - 0.548\delta_i^5) \tag{14}$$

where $\delta_i = L_c/L_i$, for $L_c \le L_i$ and $\delta_i = L_i/L_c$, for $L_c > L_i$; $D_{h,i} = 2L_cL_i/(L_t + L_c)$, $\mathrm{Re}_{Dh,i} = u_i D_{h,i}\rho_i/\mu_i$ and i = 1,7. According to Bejan (1995), the correlations used for the turbulent regime are

$$f_i = 0.079\,\mathrm{Re}_{Dh,i}^{-1/4} \qquad (2300 < \mathrm{Re}_{Dh,i} < 2\mathrm{x}10^4) \tag{15}$$

$$\frac{h_i D_{h,i}}{k_i} = \frac{(f_i/2)(D_{h,i} - 10^3)\,\mathrm{Pr}_i}{1 + 12.7(f_i/2)^{1/2}(\mathrm{Pr}^{2/3} - 1)} \qquad (2300 < \mathrm{Re}_{Dh,i} < 5\mathrm{x}10^6) \tag{16}$$

Assuming diffusion to be the dominant transport mechanism across the diffusion and catalyst layer (Bird *et al.*, 2002), the fuel and oxidant mass fluxes are given by

$$j_i = -\left[D(\rho_{out} - \rho_{in})/L\right]_i \tag{17}$$

Where, according to Newman (1991), $D = B\left\{\left[8\bar{R}T/\pi M\right]^{1/2}\phi^q\right\}$, is the Knudsen diffusion coefficient. Therefore

$$P_{i,out} = P_{i,in} - \frac{j_i R_k T_\infty L_i \theta_i}{D_i p_\infty}, \quad i = 2,6;\ k = f,ox \tag{18}$$

The net heat transfer rates at CV2 are $\tilde{Q}_2 = -\tilde{Q}_{12} + \tilde{Q}_{w2} + \tilde{Q}_{23} + \tilde{Q}_{2ohm}$, where $\tilde{Q}_{23} = \tilde{k}_{s,a}(1-\phi_2)\tilde{A}_s(\theta_2 - \theta_3)/\left[(\xi_2 + \xi_3)/2\right]$, where the subscript s,a indicates the solid anode side. The energy balance for the CV2 is:

$$(\theta_1 - \theta_2) + \frac{\tilde{Q}_2}{\psi_{H_2}} = 0 \tag{19}$$

The chemical reaction that occurs at the anode reaction layer (CV3) in an AMFC is,

$$H_2 + 2OH^- \rightarrow 2H_2O + 2e^- \tag{20}$$

The dimensionless enthalpy of formation is defined by $\tilde{H}_i = \dot{n}_i H_i/\left(\dot{m}_{ref} c_{p,f} T_\infty\right)$, where the subscript i refers to a substance or a control volume, H is the enthalpy of formation, kJ/kmol. The enthalpy change due to the anode reaction is given by $\Delta H_3 = \sum_{products}\left[\upsilon_i H_i(T_i)\right] - \sum_{reactants}\left[\upsilon_i H_i(T_i)\right]$ and $W_{e3} = -\Delta G_3$, where υ is the reaction stoichiometric coefficient, W_{e3} is the reversible work done by the CV3, J. The reaction Gibbs free energy change, ΔG, is a function of temperature, pressure and concentrations (Masterton and Hurley, 1997).

$$\Delta G = \Delta G^0 + \bar{R}T\ln Q \tag{21}$$

where $\bar{R}$ is the universal gas constant, 8.314 kJ/kmolK; $\Delta G^0 = \Delta H + T\Delta S$, ΔG is the molar Gibbs free energy change, kJ/kmol; ΔH is the molar enthalpy change, kJ/kmol; ΔS is the molar entropy change kJ/kmol; the superscript "0" indicate standard conditions (gases at 1 atm, 25°C, species in solution at 1 M), Q is the reaction quotient. In the present reaction , Eq. (18) the resulting expression for Q_3 is $Q_3 = \left\{\left[OH^-\right]^2 p_{H_2}\right\}^{-1}$, where $\left[OH^-_{(aq)}\right]$ is the molar concentration of the alkaline solution, (mol l^{-1}), and $p_{H_2} = p_{2,out}$, i.e. the H_2 partial pressure in atmospheres at the CV2 outlet. The dimensionless net heat transfer in CV3 is given by $\tilde{Q}_3 = -\tilde{Q}_{23} + \tilde{Q}_{w3} + \tilde{Q}_{34} + \tilde{Q}_{3ohm}$. The heat transfer rate between

CV3 and CV4 (alkaline membrane) is dominated by conduction, therefore $\widetilde{Q}_{34} = -(1-\phi_3)(\theta_3-\theta_4)\widetilde{A}_s 2\widetilde{k}_{s,a}\widetilde{k}_m/(\xi_4\widetilde{k}_{s,a}+\xi_3\widetilde{k}_m)$, where $\widetilde{k}_m$ is the dimensionless thermal conductivity of the membrane (CV4). The mass and energy balances for CV3 is

$$\widetilde{Q}_3 - \Delta\widetilde{H}_3 + \Delta\widetilde{G}_3 = 0 \tag{22}$$

where, $(\Delta\widetilde{H}_3, \Delta\widetilde{G}_3) = \dot{n}_{H_2}(\Delta H_3, \Delta G_3)/\left(\dot{m}_{ref} c_{p,f} T_\infty\right)$.

The dimensionless net heat transfer in CV4 is obtained from $\widetilde{Q}_4 = -\widetilde{Q}_{34} + \widetilde{Q}_{w4} + \widetilde{Q}_{45} + \widetilde{Q}_{4ohm}$ and $\widetilde{Q}_{45} = -(1-\phi_5)(\theta_4-\theta_5)\widetilde{A}_s 2\widetilde{k}_{s,c}\widetilde{k}_m/(\xi_4\widetilde{k}_{s,c}+\xi_5\widetilde{k}_m)$. Next, the CV4 temperature is obtained from

$$\widetilde{Q}_4 + \widetilde{H}(\theta_5)_{OH^-} - \widetilde{H}(\theta_4)_{OH^-} - \widetilde{H}(\theta_3)_{H_2O} - \widetilde{H}(\theta_4)_{H_2O} = 0 \tag{23}$$

In the cathode reaction layer (CV5), the following reaction occurs

$$\frac{1}{2}O_2 + 2H_2O + 2e^- \rightarrow 2OH^- \tag{24}$$

The CV5 dimensionless temperature is obtained by

$$\widetilde{Q}_5 - \Delta\widetilde{H}_5 + \Delta\widetilde{G}_5 = 0 \tag{25}$$

where $(\Delta\widetilde{H}_5, \Delta\widetilde{G}_5) = \dot{n}_{O_2}(\Delta H_5, \Delta G_5)/\left(\dot{m}_{ref} c_{p,f} T_\infty\right)$.

Similarly, the dimensionless net heat transfer rate flowing in CV5 is given by $\widetilde{Q}_5 = -\widetilde{Q}_{45} + \widetilde{Q}_{w5} + \widetilde{Q}_{56} + \widetilde{Q}_{5ohm}$, with $\widetilde{Q}_{56} = -\widetilde{k}_{s,c}(1-\phi_6)\widetilde{A}_s(\theta_5-\theta_6)/\left[(\xi_5+\xi_6)/2\right]$.

The enthalpy change during cathode reaction is $\Delta H_5 = \sum_{products}\left[\upsilon_i H_i(T_i)\right] - \sum_{reactants}\left[\upsilon_i H_i(T_i)\right]$, while $W_{e5} = -\Delta G_5$. The CV5 reaction quotient is $Q_5 = \left[OH^-\right]^2/p_{O_2}^{1/2}$, where $p_{O_2} = p_{6,out}$.

The dimensionless net heat transfer rate in CV6 results from $\widetilde{Q}_6 = -\widetilde{Q}_{56} + \widetilde{Q}_{w6} + \widetilde{Q}_{67} + \widetilde{Q}_{6ohm}$, with $\widetilde{Q}_{67} = \widetilde{h}_7\widetilde{A}_s(1-\phi_6)(\phi_7-\phi_7)$, $\widetilde{h}_7 = h_7 V_T^{2/3}/\left(\dot{m}_{ref} c_{p,f}\right)$. The dimensionless temperature for CV6 is given by

$$\widetilde{Q}_6 + \psi_{O_2}\frac{c_{p,ox}}{c_{p,f}}(\theta_7-\theta_6) + \widetilde{H}(\theta_5)_{H_2O} - \widetilde{H}(\theta_6)_{H_2O} = 0 \tag{26}$$

The dimensionless net heat transfer rate in CV7 is $\widetilde{Q}_7 = -\widetilde{Q}_{67} + \widetilde{Q}_{w7} + \widetilde{Q}_{7ohm}$. The balances for mass and energy in the oxidant channel (CV7), the assumptions of non-mixing flow, and the assumption that the space is filled mainly with dry oxygen, yield $\dot{m}_{H_2O} = \dot{m}_{H_2O,in} = \dot{m}_{H_2O,out} = \dot{n}_{O_2} M_{H_2O}$ and

$$\widetilde{Q}_7 + \psi_{ox}\frac{c_{p,ox}}{c_{p,f}}(\theta_{ox}-\theta_7) + \widetilde{H}(\theta_6)_{H_2O} - \widetilde{H}(\theta_7)_{H_2O} = 0 \tag{27}$$

2.2. Electrochemical model

Based on the electrical conductivities and geometry of each compartment, the electrical resistances, $\beta(\Omega)$, are given by:

$$\beta_i = \frac{\xi_i}{\widetilde{A}_s V_T^{1/3}\sigma_i(1-\phi_i)}, \qquad i = 1,2,6,7 \tag{28}$$

$$\beta_i = \frac{\xi_i}{\widetilde{A}_s V_T^{1/3}\sigma_i\phi_i}, \qquad i = 3, 4, 5, \ (\phi_4 = 1) \tag{29}$$

Where $\sigma_i = \sigma_{solution} = -2.041M - 0.0028M^2 + 0.005332MT_i + 207.2MT_i^{-1} + 0.001043M^3 - 3.10^{-7}MT^2$ for i=3,4,5; where T is the temperature, K and M is the molarity of the alkaline solution, mol/L (Gilliam *et al.*,2007). The conductivities of the diffusive layer, σ_2 and σ_6, are the carbon-phase conductivities (Kulikovsky, 2000). Finally, the conductivities of CV1 and CV7, σ_1 and σ_7, are given by the electrical conductivity of the bipolar plate material.

The appropriate figure of merit for evaluating the performance of a fuel cell is the polarization curve, i.e., the fuel cell total potential as a function of current. The dimensionless potential is defined in terms of a given reference voltage, V_{ref}, namely $\widetilde{V} = V/V_{ref}$ and $\widetilde{\eta} = \eta/V_{ref}$, where V is the voltage of the fuel cell, V; η is the overpotential, V; $\widetilde{\eta}$ is the dimensionless overpotential, and $\widetilde{V}$ is the dimensionless voltage of the fuel cell. The dimensionless actual potential $\widetilde{V}_i$ is an accumulated result of dimensionless irreversible anode electrical potential $\widetilde{V}_{i,a}$, dimensionless irreversible cathode electrical potential $\widetilde{V}_{i,c}$, and the dimensionless ohmic loss $(\widetilde{\eta}_{ohm})$ in the space from CV1 to CV7, i.e.,

$$\widetilde{V}_i = \widetilde{V}_{i,a} + \widetilde{V}_{i,c} - \widetilde{\eta}_{ohm} \tag{30}$$

The ohmic loss $\widetilde{\eta}_{ohm}$ is estimated by $\widetilde{\eta}_{ohm} = \frac{I}{V_{ref}}\sum_{i=1}^{7}\beta_i$. The reversible electrical potential at the anode is given by the Nernst equation, $V_{e,a} = V_{e,a}^{o} - \frac{\overline{R}T_3}{nF}\ln Q_3$. Where $V_{e,a} = \Delta G_3/(-nF)$ and $V_{e,a}^{o} = \Delta G_3^{o}/(-nF)$. At the anode there are two mechanisms for potential losses; (i) charge transfer, and (ii) mass diffusion. The potential loss at the anode (η_a) due to charge transfer is obtained implicitly from the Butler-Volmer equation for a given current I (Gurau *et al.*,2000); $\frac{I}{A_{3,wet}} = i_{o,a}\left\{\exp\left[\frac{(1-\alpha_a)\eta_a F}{\overline{R}T_3}\right] - \exp\left[-\frac{\alpha_a\eta_a F}{\overline{R}T_3}\right]\right\}$; where α_a is the anode charge transfer coefficient and $i_{o,a}$ is the anode exchange current density. The potential loss due to mass diffusion is $\eta_{d,a} = \frac{\overline{R}T_3}{nF}\ln\left(1 - \frac{I}{A_{3,wet}i_{Lim,a}}\right)$, $i_{lim,a} = \frac{p_f D_2 nF}{M_{H_2}L_2R_f\theta_2T_\infty}$. The resulting electrical potential at the anode is $\widetilde{V}_{i,a} = \widetilde{V}_{e,a} - \widetilde{\eta}_a - |\widetilde{\eta}_{d,a}|$.

The methodology in estimating the anode potential is valid in building the cathode potential correlations. Similarly, the actual cathode potential is $\widetilde{V}_{i,c} = \widetilde{V}_{e,c} - \widetilde{\eta}_c - |\widetilde{\eta}_{d,c}|$ and the reversible electrical cathode potential is $V_{e,c} = V_{e,c}^{o} - (\overline{R}T_5/nF)\ln Q_5$, where $V_{e,c}^{o} = \Delta G_5^{o}/(-nF)$. The Butler-Volmer equation for calculating the cathode side overpotential η_c is $I/A_{5,wet} = i_{o,c}\left[\exp((1-\alpha_c)\eta_c F/(\overline{R}T_5)) - \exp(\alpha_c\eta_c F/(\overline{R}T_5))\right]$where α_c is the cathode charge transfer coefficient, and $i_{o,c}$ is the cathode exchange current density. The cathode mass diffusion depleting overpotential is $\eta_{d,c} = \overline{R}T_5/(nF)\ln(1 - I/(A_{5,wet}i_{Lim,c}))$, and the cathode limiting current density is $i_{lim,c} = 2p_{ox}D_6nF/(M_{O_2}L_6R_{ox}\theta_6T_\infty)$.

The pumping power $\widetilde{W}_p$ is required to supply the fuel cell with fuel and oxidant. Therefore the total net power (available for utilization) of the fuel cell is $\widetilde{W}_{net} = \widetilde{W} - \widetilde{W}_p$; where $\widetilde{W} = \widetilde{V}_i\widetilde{I}$ is the total fuel cell electrical power output, $\widetilde{W}_p = \psi_f S_f\frac{\theta_i}{Pi}\Delta P_1 + \psi_{ox}S_{ox}\frac{\theta_7}{P_7}\Delta P_7$ and $S_f = \frac{m_{ref}T_\infty R_i}{V_{ref}I_{ref}}$, i = f,ox.

3. NUMERICAL RESULTS OF AMFC MODEL

The numerical results were obtained solving the system of equations (7), (18), (19), (22), (23), (25), (26) and (27) presented in the previous section with a FORTRAN code, using a quasi-Newton method. The single AMFC net power output depends on the internal structure and the external shape of the fuel cell. The mathematical model allows the computation of the total net power of the fuel cell, which is possible to be done as soon as the physical values and a set of geometric internal and external parameters are known. In the case of the present study, such set is given by Tab. 1.

Important parameters were varied starting from the reference case shower on Table 1. The variation of two design parameters (the porosity of the reactive layer of electrodes ϕ_3, ϕ_5 and of the membrane ϕ_4) and operational parameters (temperature of the feeding gases) on the AMFC performance has been considered and is shown on the following figures.

Table 1. Physical properties used as reference case in the numerical solution.

B = 0.156	$p_f = p_{ox} = p_\infty = 0.1\text{MPa}$
$c_{p,f}$ = 14.95 kJ kg^{-1} K^{-1}	q = 2.1
$c_{p,ox}$ = 0.91875 kJ kg^{-1} K^{-1}	R_f = 4.157 kJ kg^{-1} K^{-1}
$c_{v,f}$ = 10.8 kJ kg^{-1} K^{-1}	R_{ox} = 0.2598 kJ kg^{-1} K^{-1}
$c_{v,ox}$ = 0.659375kJ kg^{-1} K^{-1}	T_∞ = 290.15 K
I_{ref} = 1 A	U_{wi} = 50 W m^{-2} K^{-1}, i = 1 to 7
k_f = 0.1805 W m^{-1} K^{-1}	V_{ref} = 1 V
k_{ox} = 0.0266 W m^{-1} K^{-1}	$V_T = 7.69\times10^{-5}$ m^3
k_p = 0.12 W m^{-1} K^{-1}	$\alpha_a, \alpha_c = 0.5$;
$K_2, K_6 = 4 \times 10^{-10}$ m^2	$\zeta_1, \zeta_7 = 2$
$K_3, K_5 = 4 \times 10^{-12}$ m^2	$\mu_1 = 10^{-5}$ Pa.s
$\dot{m}_{ref} = 10^{-3}$kg s^{-1}	$\mu_7 = 2.4\times10^{-5}$ Pa.s
M = 6.9 mol/L	

Since it was assumed that the same electrode type, a Pt/C based electrode was used in both sides of the AMFC, was considered $\phi_3 = \phi_5$. Fig. 3 shows the results for power curve for different values of porosity and maximum power as function of porosity for different inlet gas temperatures. The range analyzed was from $0.03 \le \phi_3 = \phi_5 < 1$ and $293.15\text{ K} \le T_f = T_{ox} \le 333.15\text{ K}$.

As can be seen in the Fig. 3a the higher the porosity of the catalytic layers, more effective an electrode will be, as expected. Since more solution will be absorbed and also a bigger superficial area would be available for the electrochemical reaction occur. However there are physical constraints in the electrode manufacturing process that determine a maximum porosity for the catalytic layers.

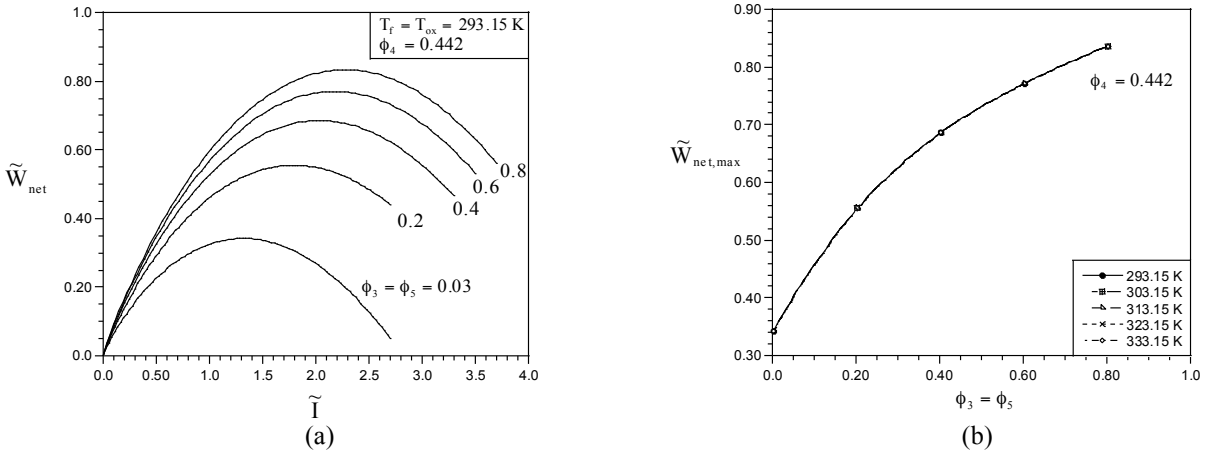

Figure 3. (a) Power curves for different values of electrode porosity; (b) Maximum power produced for different values of electrode porosity and inlet temperature of fuel and oxidant ($T_f = T_{ox}$).

According to the Fig. 3b the increase of temperature of the inlet gases has no influence on the maximum net power produced, which indicates that the porosity of the electrodes (ϕ_3 and ϕ_5) plays a key role in the achievement of higher maximum net power, as can be seen in the Fig. 3a. The fuel cell type studied on this paper has a differential which is solid support that enhances the feasibility of alkaline fuel cells use. From the results shown on Fig. 4 it can be concluded that for the case studied it isn't necessary a high porosity for this solid support, for values higher than $\phi_4 = 0.20$ the maximum net power decreases until $\phi_4 = 0.60$ where it has a slight increase however not exceeding the maximum net power reached at $\phi_4 = 0.20$.

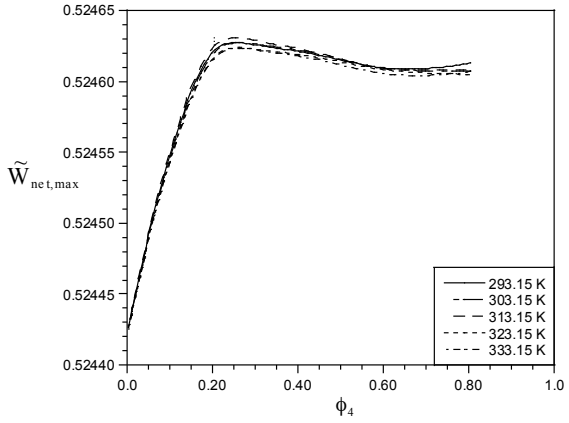

Figure 4. Parametric Analysis of the influence of the porosity of the solid membrane support porosity on the maximum power produced for AMFC for $\phi_3 = \phi_5 = 0.2$.

The parametric analysis was made aiming a better understanding of how those parameters affect the power output of the fuel cell. As a future study those results will be used as a tool for power optimization.

5. ACKNOWLEDGEMENTS

Acknowledgments for the Center for Advanced Power systems at Florida State University, AFOSR (Award No. FA9550-06-1-0527), the Brazilian National Council of Scientific and Technological Development, CNPq (projects 578066/2008-4 and 485651/2007-6), CAPES (projects 200/2007 and 2424/11-8), and the Mechanical Engineering Graduate Program (PGMEC) of the Federal University of Parana.

6. REFERENCES

Bard, A., 1973. Encyclopedia of electrochemistry of the elements. M. Dekker, New York.

Bejan, A., 1995. Convection Heat Transfer, 2nd ed. Wiley, New York.

Bird, R. B., Stewart, W. E., Lightfoot ,E. N., 2002. Transport Phenomena, 2nd ed. Wiley, New York.

Gilliam, R. J., Graydon, J. W., Kirk, D. W., Thorpe, S. J., 2007, "A review of specific conductivities of potassium hydroxide solutions for various concentrations and temperatures". Internatinal Journal of Hydrogen Energy, Vol 32, pp.359-364.

Gurau ,V., Barbir, F., Liu, H., 2000, "An analitical solution of a half-cell model for PEM fuel cells". J. Electrochem. Soc., Vol. 147, pp 2468-2477.

Kincaid, D., Cheney, W., 1991. Numerical Analysis Mathematics of Scientific Computing, 1st ed., Wadsworth, Belmont, CA.

Kulikovsky, A. A., Divisek ,J., Kornyshev, A. A., 2000, "Two-dimensional simulation of direct methanol fuel cells –a new (embedded) type of current collector". J. Electrochem. Soc. , Vol. 147, pp. 953-959.

Masterton, W. L., Hurley, C. N., 1997. Chemistry Principles & Reactions, 3rd ed., Saunders College Publishing, Orlando, FL.

Newman, J. S., 1991. Electrochemical Systems, 2nd ed., Prentice Hall, Englewood Cliffs, NJ, pp. 255, 299, 461.

O'Hayre, R., Cha, S., Colella, W., Prinz, F. B., 2006. Fuel Cell Fundamentals, 2nd ed., Wiley, New Jersey.

Shah, R. K., and London, A. L. , 1978. " Laminar Flow Forced Convection in Ducts, Supplement 1 to Advances in Heat Transfer", Academic Press, New York.

Sommer, E.M., Martins, L.S., Vargas, J.V.C., Gardolinski, J.E.F.C., Ordonez, J.C., Marino, C.E.B., 2012. "Alkaline Membrane Fuel Cell (AMFC) modeling and experimental validation". Journal of Power Sources, Vol. 213, pp. 16-30.

Vargas, J. V. C. ; Gardolinski, J. E. F. C.; Ordonez, J. C. Hovsapian, R. ALKALINE MEMBRANE FUEL CELL. Patent, USPTO application number 61/067,404 – 2008.

7. RESPONSIBILITY NOTICE

The authors are the only responsible for the printed material included in this paper.